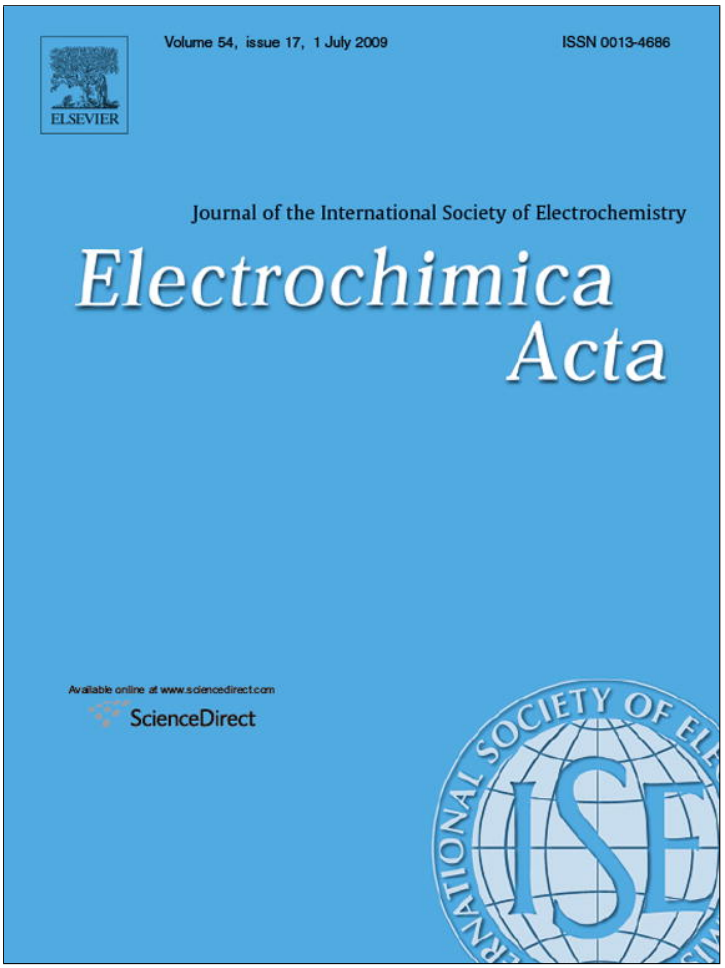

Electrochimica Acta 54 (2009) 4192–4197

Contents lists available at ScienceDirect

Electrochimica Acta

journal homepage: www.elsevier.com/locate/electacta

Spontaneous adsorption of 3,5-bis(3,5-dinitrobenzoylamino) benzoic acid onto carbon

Julieta I. Paez[a], Miriam C. Strumia[a], Mario C.G. Passeggi Jr.[b], Julio Ferrón[b,c], Ana M. Baruzzi[d], Verónica Brunetti[d,*]

[a] Departamento de Química Orgánica (IMBIV-CONICET), Facultad de Ciencias Químicas, Universidad Nacional de Córdoba, Córdoba (5000), Argentina
[b] Laboratorio de Superficies e Interfaces (INTEC-CONICET), Facultad de Ingeniería Química, Universidad Nacional del Litoral, Santa Fe (3000), Argentina
[c] Departamento de Materiales, Facultad de Ingeniería Química, Universidad Nacional del Litoral, Santa Fe (3000), Argentina
[d] Departamento de Fisicoquímica (INFIQC-CONICET), Facultad de Ciencias Químicas, Universidad Nacional de Córdoba, Córdoba (5000), Argentina

ARTICLE INFO

Article history:
Received 22 September 2008
Received in revised form 17 February 2009
Accepted 22 February 2009
Available online 6 March 2009

Keywords:
Dendron
Immobilization
Self-assembly
Glassy carbon electrodes
Functionalized electrodes

ABSTRACT

Dendritic molecules contain multifunctional groups that can be used to efficiently control the properties of an electrode surface. We are developing strategies to generate a highly functionalized surface using multifunctional and rigid dendrons immobilized onto different substrates. In the present work, we explore the immobilization of a dendritic molecule: 3,5-bis(3,5-dinitrobenzoylamino) benzoic acid (D-NO_2) onto carbon surfaces showing a simple and rapid way to produce conductive surfaces with electroactive chemical functions. The immobilized D-NO_2 layer has been characterized using atomic force microscopy and cyclic voltammetry. D-NO_2 adsorbs onto carbon surfaces spontaneously by dipping the electrode in dendron solutions. Reduction of this layer generates the hydroxylamine product. The resulting redox-active layer exhibits a well-behaved redox response for the adsorbed nitroso/hydroxylamine couple. The film permeability of the derivatized surface has been analyzed employing the electrochemical response of redox probes: $Ru(NH_3)_6^{3+}/Ru(NH_3)_6^{2+}$ and $Fe(CN)_6^{3-}/Fe(CN)_6^{4-}$. Electrocatalytic oxidation of nicotinamide adenine dinucleotide onto a modified carbon surface was also observed.

1. Introduction

Self-assembled monolayers (SAMs) represent an extremely versatile tool for modifying sensor surfaces. In particular, self-organized molecular layers combining both structural and functional control could be a key concept for the development of new materials. Dendrons and dendrimers are precisely quantized, three-dimensional nanostructures that offer such control and provide a promising route for constructing new nanodevices and optimizing nanosensors [1–4]. The monodisperse nature of dendrons and dendrimers makes them important for nanoscientists. They are unlike traditional polymers in which critical nanoscale parameters, such as size, shape, and functionality, can be precisely controlled through their architecture, i.e. their cores, interiors, and surfaces [5].

For the purpose of taking advantage of the specific structure of dendritic macromolecules to enrich the area of SAMs, recently several specific dendrimers have been studied to fabricate organic thin films [6–8]. Particularly, dendrimers and dendrons are of great interest to both nano and polymer scientist as building blocks due to their unique, architecturally driven, macromolecular properties [9–13]. By having a high density of functional groups on their surfaces, dendrimers and dendrons are useful as spacers or linkers between surfaces of solid supports and biological macromolecules, such as peptides, proteins, antibodies, and DNA strands [14–17]. In addition, using dendritic molecules can increase the selectivity of the material [18]. The developments of useful (bio)functionalization methodologies, as well as the incorporation of novel materials having unique properties, are subjects of intensive studies. In particular, the fourth-generation poly(amidoamine) (G4-PAMAM), a highly branched dendritic macromolecule with a particle size of ca. 5 nm and 64 surface amine groups per particle, can be obtained commercially and was used in several studies for the development of biosensors [19–22].

Considering the extremely rich structural variation of dendrons and dendrimers several tailor-made surfaces could be available for pattern recognition and functional chips. Recently, self-assembled dendron thiols on gold, with a high density of peripheric-end amine groups, have been studied as a bioreactive platform useful for the immobilization of biological macromolecules for various biosensor applications, such as the fabrication of DNA microarrays and protein chips [23]. Different sizes of Frechet-type dendrons with a thiol group at a focal point can form patterned stripes with

* Corresponding author. Fax: +54 351 4334188.
E-mail addresses: brunetti@fcq.unc.edu.ar, verobrunetti@gmail.com (V. Brunetti).

0013-4686/$ – see front matter © 2009 Elsevier Ltd. All rights reserved.
doi:10.1016/j.electacta.2009.02.064

nanometer-sized features and long-range order when they are used for the preparation of SAMs onto metal surfaces [24]. In addition, the precisely tailored structure of dendron-thiols with local controlled hydrophobic and hydrophilic peripheries allows a nano-separation in a confined state, leading to the formation of an energetically favorable pore structure [25].

With the aim of gaining some additional insight about the chemical modification of electrode materials using dendritic molecules, [3,5-bis(3,5-dinitrobenzoylamino) benzoic acid] or (D-NO_2) has been synthesized. The dendritic molecule contains three aromatic rings in its body, four nitro groups as peripheric-ends and a carboxylic acid group as focal point. The presence of functional groups can significantly alter the nature and magnitude of the interactions between aromatic molecules and electrode surfaces. Recently, Wuest et al. reported that the energy of adsorption of 1,3,5 trinitrobenzene on carbon is close to three times greater than that of nitrobenzene, and the presence of carboxyl groups on the benzene ring dramatically increases binding to graphite [26]. In a previous work, we analyzed the attachment of D-NO_2 on gold electrodes [27]. D-NO_2 adsorbs onto gold electrode surfaces by dipping the metal surface in a dendron solution overnight or via grafting of cystamine covalently attached to gold electrode. Reduction of this layer generates the hydroxylamine product with a coulometric yield estimated at around 60%. The resulting redox-active layer exhibits a well-behaved redox response for the adsorbed nitroso/hydroxylamine couple [27].

Carbon electrodes are widely used in electrochemical applications due to their relatively low cost compared to other electrodes (for example, gold or platinum). Glassy carbon is popular as an electrode material due to its excellent mechanical and electrical properties, wide usable potential range and relatively reproducible performance [28]. Modification of the carbon surface is an important objective in electrochemistry and material science and provides a promising route to achieve in a simple way new materials for electrocatalysis or biosensing platforms. In the present paper, assuming that π–π interactions should favor the adsorption onto carbon surfaces, we explore the immobilization by direct adsorption of D-NO_2 onto glassy carbon (GCE) and highly ordered pyrolytic graphite (HOPG) electrodes. Cyclic voltammetry has been used as the electrochemical probe to characterize the derivatized surface. The dendron attachment was followed through the observation of the electrochemical signal of reporting groups such as the nitro one. A comparative analysis with literature data, and a "fingerprinting" by comparison of the voltammetry of the electrochemical reduction of an aryl-nitro moiety in aqueous solution was made. Modified surfaces were studied through Atomic Force Microscopy (AFM). Diffusion controlled redox couples such as $Ru(NH_3)_6^{3+/2+}$ and $Fe(CN)_6^{3-/4-}$ were employed to analyze the blocking properties of the D-NO_2 layer coated. Lastly, electrocatalytical oxidation toward NADH was evaluated.

2. Experimental

2.1. Materials

3,5-Dinitrobenzoyl chloride (Fluka, 98%) was used as received; N,N-Dimethyladetamide (DMAc, Tedia) was dried over 0.4 nm molecular sieves; and 3,5-diaminobenzoic acid (Aldrich, 98%) was purified by recristallization from water. The synthesis of dendron (3,5-bis(3,5-dinitrobenzoylamino) benzoic acid) or (D-NO_2) (see Scheme 1) was obtained following the Kakimotoĭs procedure [29–31] by using 3,5-diaminobenzoic acid and 3,5-dinitrobenzoyl chloride in DMAc. The rest of commercially available chemicals were reagent grade and were used without further purification. All solutions were prepared immediately prior to their use. Phosphate buffer solutions used in this work contained 0.1 M Na_2HPO_4/NaH_2PO_4. Water was purified with a Millipore Milli-Q system.

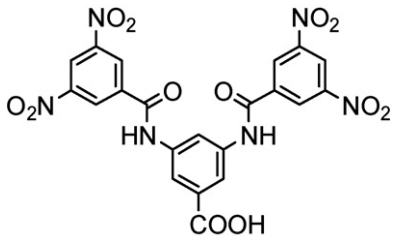

Scheme 1. Schematic representation of D-NO_2: 3,5-bis(3,5-dinitrobenzylamine benzoic acid).

2.2. Glassy carbon electrodes preparation

Prior to its modification, the GCE (CH Instruments, Inc. Austin, TX) of 3.0 mm diameter were polished using 1, 0.3 and 0.05 mm alumina (Buehler) and rinsed with water and ethanol. After its polishing, the electrodes were sonicated for 10 min in distilled water and dried in a N_2 flux. GCE were incubated in a dimethylsulfoxide (DMSO) solution containing 1–10 mM of D-NO_2 for times varying from 5 seconds to overnight. Following the modification, the derivatized surface (D-NO_2/GCE) was subsequently rinsed with copious volumes of ethanol and water, and employed immediately after its preparation.

2.3. Electrochemical measurements

All electrochemical measurements were performed at room temperature with an Autolab electrochemical analyzer and a conventional three-electrode system, comprising a carbon working one, a platinum foil as the auxiliary, and a Ag/AgCl 3.0 M NaCl electrode (from BAS) as the reference. All potentials were reported versus the Ag/AgCl reference electrode at room temperature. Nitrogen gas was used to deaerate all aqueous solutions before their use.

2.4. Atomic force microscopy (AFM)

AFM Images were acquired with a commercial Nanotec Electronic System operating in tapping mode at an atmosphere pressure and room temperature. Acquisition and image processing were performed using the WS × M free software [32]. Budget Sensors Multi75E cantilevers with an electrically conductive coating of 5 nm chromium and 25 nm platinum on both sides of the tip, resonance frequency in the range of 60–90 kHz, nominal force constant in the range of 1–7 N/m and radius smaller than 25 nm, were used. The reason for using conductive tips involves additional measurements of Kelvin Probe Force Microscopy that are in progress. The samples for AFM analysis were prepared by immersing freshly cleaved HOPG in a Dimethylsulfoxide (DMSO) solution containing 1–10 mM of D-NO_2. Samples were subsequently rinsed with copious volumes of ethanol and water, dried under nitrogen flux and analyzed immediately.

3. Results and discussion

3.1. Voltammetric characterization of D-NO_2/GCE

Fig. 1 shows cyclic voltammograms recorded from -0.8 to 0.6 V versus Ag/AgCl for a D-NO_2 modified GCE (by self-assembly) in phosphate buffer solution (pH 7) at 0.1 V s^{-1}. The initial potential was set at −0.2 V, scanning in the positive direction until 0.6 V

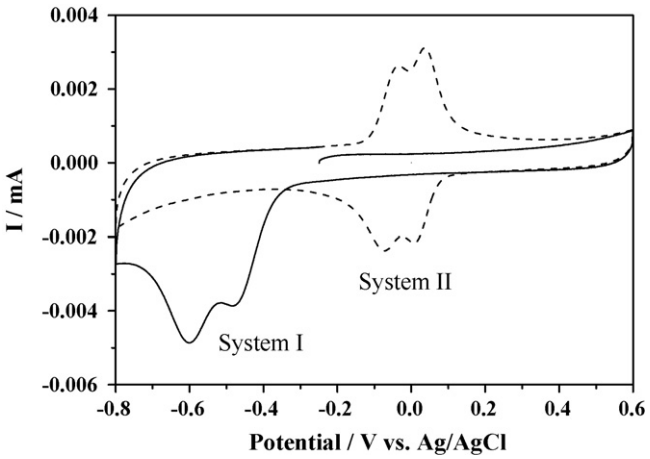

Fig. 1. Cyclic voltammograms at 0.1 V s^{-1} for a D-NO_2/GCE in 0.1 M phosphate buffer (pH 7). First (solid line) and second (dashed line) scan.

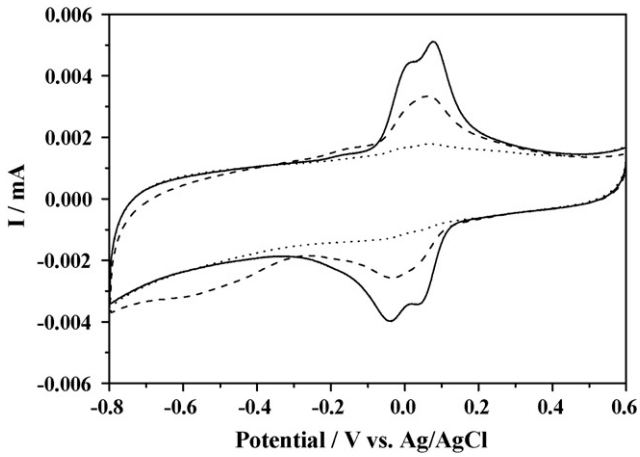

Fig. 2. Cyclic voltammograms at 0.1 V s^{-1} for a D-NO_2/GCE in 0.1 M phosphate buffer (pH 7) upon continuous cycling in the potential range from −0.8 to 0.6 V. Second (solid line) and 50th (dashed line) scan. Bare GCE (dotted line) is shown for comparison.

without the appearance of any faradaic process. In the reductive direction, two large reduction waves labeled as system I are observed between −0.4 and −0.7 V. Two oxidative waves are observed at more positive potentials, ca. 0.5 V, than the reduction potential of system I, which appear only if the cathodic switching potential reaches −0.5 V. Once the oxidative processes appear, the corresponding reduction peaks appear at 0.020 V and −0.080 V, respectively. This is indicative that system I is electrochemically irreversible and that the new system, labeled as system II, is electrochemically quasi-reversible. Although the electrochemical behavior of D-NO_2 adsorbed onto GCE is qualitatively similar to that previously reported on gold [27], two important differences are found. For each system (I and II), the appearance of two waves instead of one is observed and the self-assembly of D-NO_2 onto GCE is reached in a few minutes instead of the long time of incubation (more than 12 h) observed for gold surfaces. In addition, the amount of surface active nitro groups is much higher than when the electrode is modified with the precursor (3,5-dinitrobenzoic acid) by self-assembly (see Supplementary Information). It is important to point out that the voltammetry of nitrobenzene and nitrosobenzene physisorbed onto different substrates [33–37] is indeed characteristic of the electrochemical reduction of an aromatic nitro compound and it is consistent with the general mechanism previously described by Compton et al. [35,36]. By analogy, in our case system I should correspond to the four-electron reduction of each nitro moiety to the corresponding aryl hydroxylamine. On the subsequent positive-going sweep, system II can be attributed to the two-electron oxidation/reduction of the aryl-hydroxylamine/aryl-nitroso moieties. The charge corresponding to system I (0.25 mC cm^{-2}) is in good agreement with that associated with system II during the second scan (0.15 mC cm^{-2}), as expected from the ratio of stoichiometries of reactions 1 and 2. The nature of two waves instead of one in the scans for each system (I and II) will be discussed further on.

Fig. 2 shows cyclic voltammograms for D-NO_2/GCE upon continuous cycling in 0.1 M phosphate buffer solutions (pH 7). The subsequent voltammograms give rise essentially to the same electrochemical behavior of System II but the two waves join in one and whereas the reduction wave decreases reaching a similar value than the oxidation wave, until a stabilized voltamperometric profile is reached. The charge decrease may be caused by desorption from the electrode of some active species during the continuous cycling. In order to characterize whether the molecules were indeed attached onto the carbon surfaces we performed the following three step procedure. First, between 30–50 multiple scans were performed on each of the modified GCE around system II until the voltammetric response was found to remain stable. Next, the electrode was removed, the electrolyte solution was replaced with fresh solution and a new scan performed. In every case, the observed voltammogram was found to overlay the previous scans, indicating that the redox-active species are only present on the electrode surface. Finally, the scan rate was varied from 0.05 up to 0.225 V s^{-1} as shown in Fig. 3. The inset illustrates the scan rate dependence of the peak current density. For both, the cathodic and anodic peak currents, $I_{p,c}$ and $I_{p,a}$ respectively, a linear dependence on the sweep rate v was found indicating that the molecules adsorbed on the surface constitute a surface-confined redox pair.

To provide us a further insight into the presence of two cathodic current peaks for system I and two anodic and their corresponding cathodic waves for system II instead of only one, as expected for reaction 1 and 2, respectively, voltammograms were carried out increasing the negative potential limit progressively. Fig. 4 shows the effect of the lower switching potential. When the onset of the first wave was reached (ca. −0.5; cathodic peak A), the quasi-reversible couple appears centered at 0.0 V. On the second scan, sweeping the potential to more negative values results in the generation of the cathodic current peak B which is clearly associated to the couple centered at ca. −0.08 V. In addition, a voltamperogram profile obtained after repetitive cycling for system II only exhibits a

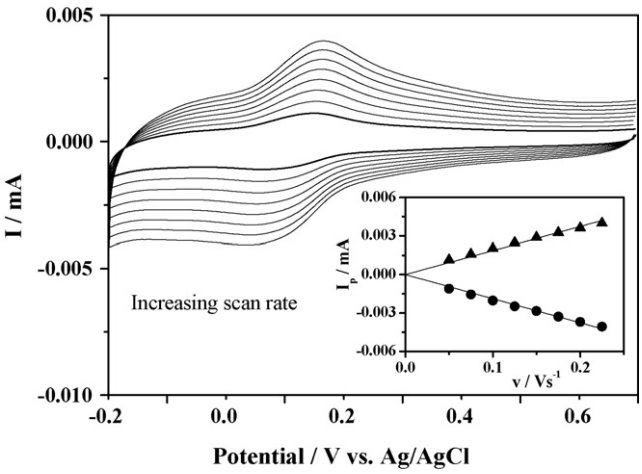

Fig. 3. Cyclic voltammograms at different sweeps rates of D-NO_2/GCE measured for the response after 50 scans in the potential range from −0.3 to 0.6 V. Inset shows plots of anodic (▲) and cathodic (●) peak current as a function of v.

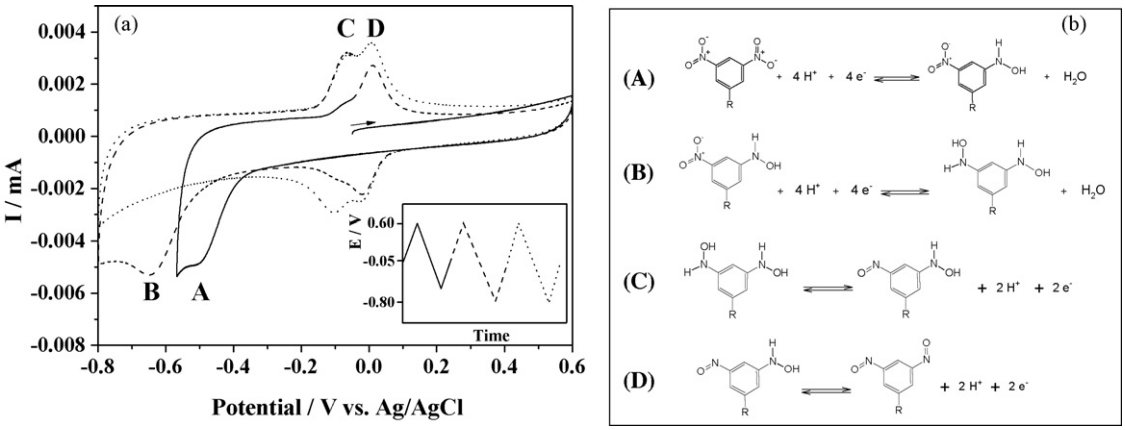

Fig. 4. (a) Electrochemical behavior of D-NO_2/GCE in 0.1 M phosphate buffer (pH 7) obtained applying the potential-time routine indicated in the inset. First (solid line), second (dashed line) and third (dotted line) scan. (b) Scheme of proposed reactions.

couple centered at 0.04 V with broad waves related to the convolution of both peaks (as the observed in Fig. 2 for the 50th scan). This behavior could be explained considering the differences in energy for the reduction of the two NO_2 substituents in each aromatic ring of D-NO_2. Assuming that cathodic peak A is associated with the reduction of one NO_2 substituents, the reduction of the second NO_2 substituents (the cathodic peak B) occurs at more negative potentials due to the disappearance of the negative inductive effect of an electron acceptor like NO_2 in the meta position [38]. The anodic peak C is related to the oxidation of one NHOH substituent, while the anodic peak D is associated to the oxidation of the other NHOH substituent, which now has a NO substituent in the meta position (see Fig. 4b).

3.2. Electrochemical response of redox probes to evaluate the film permeability of D-NO_2/GCE

The cyclic voltammetry is an important technique used to evaluate the blocking property of the layer-coated electrodes using diffusion controlled redox couples as probes [39,40]. With this purpose, we chose the $Ru(NH_3)_6^{3+}/Ru(NH_3)_6^{2+}$ couple, which undergoes a simple charge transfer process with a high rate constant, independent of the nature and concentration of the supporting electrolyte. Fig. 5a shows the cyclic voltammograms of bare GCE and D-NO_2/GCE in 2 mM hexaammineruthenium(III) chloride at a potential scan rate of 0.1 V s^{-1} in 0.1 M phosphate buffer solution (pH 7). The bare GCE shows a voltammogram for the redox couple that corresponds to a reversible diffusion controlled electron transfer reaction. There were no significant differences in the electrochemical response of the $Ru(NH_3)_6^{3+}/Ru(NH_3)_6^{2+}$ couple on D-NO_2/GCE. This behavior goes in with the redox response of the aryl-hydroxylamine/aryl-nitroso moieties (system II) indicating that the dendritic molecules attached onto the carbon surface do not block the electron transfer reaction of this redox probe.

Identical behavior was observed with the electron transfer reaction of $Fe(CN)_6^{3-}/Fe(CN)_6^{4-}$ onto modified GCE (Fig. 5b). The conducting state is nearly metallic, with small or negligible injection barrier between carbon and the conducting layer. The electron transfer between the electrochemical active species in solution and the electrode surface can occur through the defects that arise during the formation of the layer (pinholes) or by the uncovered carbon surface. On the other hand, when the redox reaction of a molecule is not accessible on the electrode, the electron transfer reaction can occur through the layer [41]. Previous studies on biphenyl and nitrophenyl films grafted on GCE after an activation treatment show a similar conductance response [41]. The modified electrodes exhibited slower electron transfer than unmodified GCE, however, after a negative potential excursion to −2.0 V vs. Ag/Ag^+, the modified electrodes exhibited much faster electron transfer kinetics, approaching those observed on bare GCE. The effect is attributed to an apparently irreversible structural change in the film which increases the rate of electron tunneling. The increase in the electron transfer rate is consistent with an increase in the electron tunneling rate through the monolayer, caused by a significant decrease in the tunneling barrier height due to the arrangement of phenyl rings into the same plane [41].

To analyze the coverage of D-NO_2 attached onto carbon surfaces, atomic force microscopy (AFM) measurements were carried out. Fig. 6 shows AFM images where bare and derivatized HOPG after incubation in 10 mM D-NO_2/DMSO solution for 15 min are compared. The morphologies of both type of surfaces, bare (Fig. 6a) and derivatized HOPG (Fig. 6c–e), are completely different. While we observe the typical HOPG terraces separated by steps, like the one

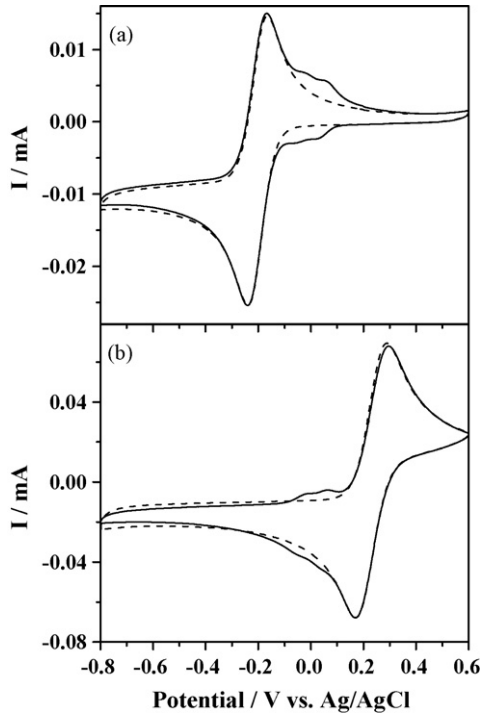

Fig. 5. Cyclic voltammograms at 0.1 V s^{-1} for a GCE in 0.1 M phosphate buffer (pH 7) containing 2 mM $Ru(NH_3)_6Cl_3$ (a) or 2 mM $K_3Fe(CN)_6$ (b) in the potential range from −0.8 to 0.6 V. GCE incubated in 10 mM D-NO_2 solution for 15 min (solid line) and bare GCE (dashed line).

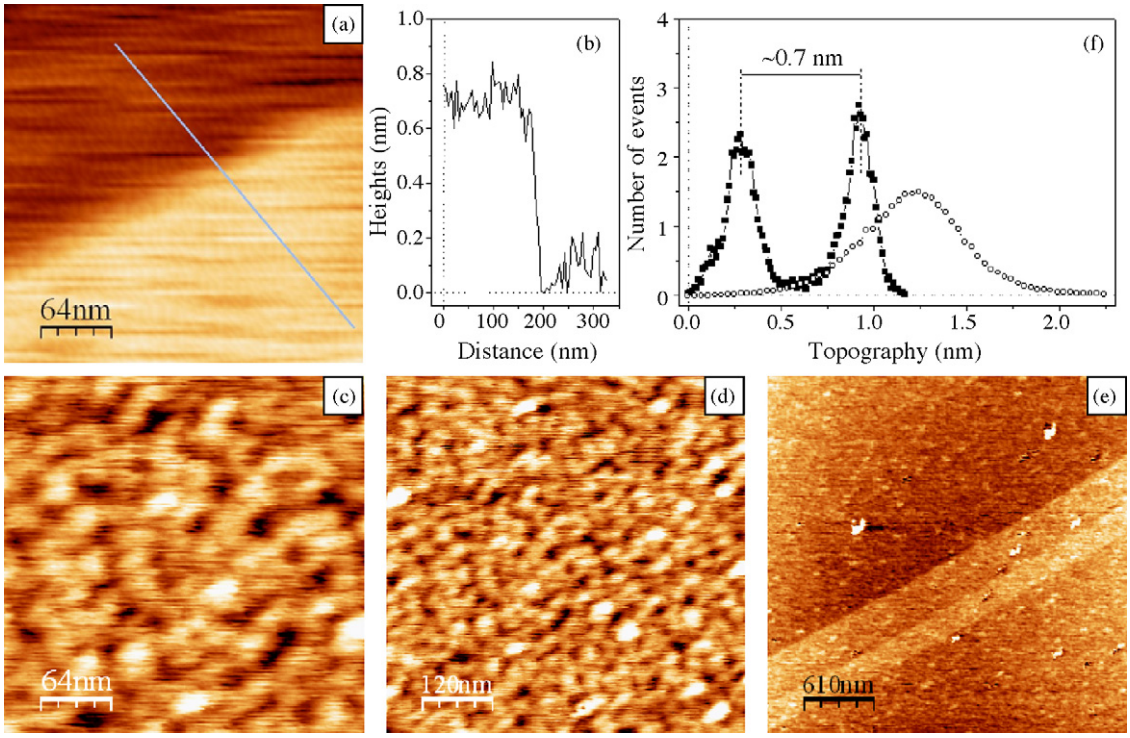

Fig. 6. AFM topographical images in tapping mode for a bare (a) and modified (c–e) HOPG after incubation in 10 mM D-NO_2 solution for 15 min. The profile shown in (a) is depicted in (b). AFM images: (a) and (c) 320 nm × 320 nm, (d) 600 nm × 600 nm, and (e) 3000 nm × 3000 nm. The comparison of roughness acquired from images (a) (■) and (c) (○) is shown in (f).

observed in Fig. 6a, whose profile (Fig. 6b) shows it as a double atomic step (~0.7 nm), the covered one shows a bubbled surface where only much more higher steps, than those observed for the bare surface, can be distinguished (see Fig. 6e). In addition, it is quite clear from the roughness analysis performed in Fig. 6f, that the one of the covered surface is larger than the bare roughness. The double peak appearing in Fig. 6f for the bare surface corresponds, each peak to the roughness of each terrace, while the difference between them is simply the step height between both terraces, shown in Fig. 6a. The analysis clearly shows that the derivatized surface obtained after 15 min of incubation (10 mM solution) is fully and homogeneously covered by the dendron. This is supported by Kelvin Probe Force Microscopy measurements, where no local contrast was observed in images for the same sample (not shown here), indicative of an electrically homogenous and, in this case, completely covered surface. AFM images for partially covered carbon surfaces can be obtained decreasing either the incubation time or the concentration of the dendron solution (see Supplementary Information).

The present results raise some interesting possibilities in electroanalysis and related areas. By using D-NO_2 modified GCE, solution species interact with a conducting organic layer rather than a graphitic or metallic surface. There is a little difference between a bare surface and the D-NO_2/GCE for the case of outer-sphere redox systems, but for any electrocatalytic process involving adsorption or interaction with surfaces sites, the modified surface may behave very differently from bare GCE. Having the chance to have a functional group (such as the nitro group), dendron modified GCE may allow variations in catalytic activity while the electron transfer still occurs.

3.3. Electrocatalysis of NADH oxidation

As stated in Section 3.1, D-NO_2 spontaneously adsorbs onto GCE by dipping the electrode in a dendron solution. Reduction of this layer generates the hydroxylamine product. The resulting redox-active layer exhibits a well-behaved redox response for the adsorbed nitroso/hydroxylamine couple. This has been shown to be important in electrocatalytic oxidation of nicotinamide adenine

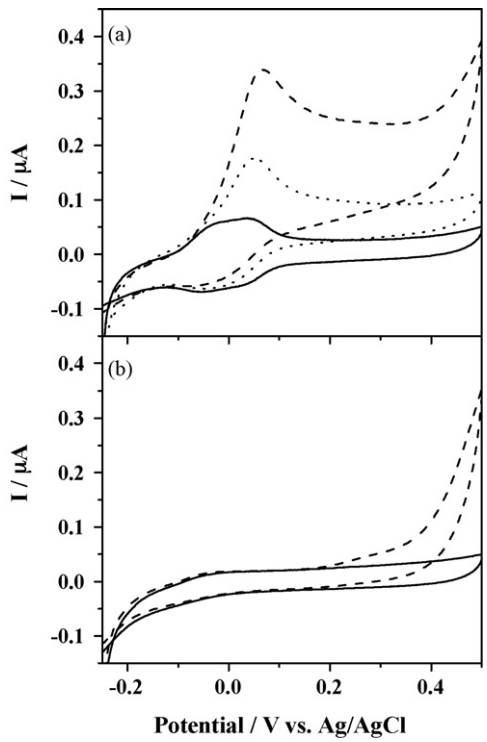

Fig. 7. (a) Electrochemical behavior of D-NO_2/GCE after cycling in 0.1 M phosphate buffer (pH 7) in the absence (solid line) and presence of NADH: 0.1 mM (dot line) and 0.5 mM (dashed line). (b) unmodified GCE in the absence (solid line) and presence (dashed line) of 0.5 mM NADH. Scan rate $v = 0.002\,V\,s^{-1}$.

dinucleotide (NADH) onto gold electrodes [33], in biosensor applications [38,42,43] and the electroanalytical explotation of nitrosophenyl modified substrate for the quantification of thiols [44,45].

To test the potential electrocatalytic activity of these materials onto GCE, the cyclic voltamperometric responses of derivatized D-NO_2/GCE were obtained in the absence and presence of NADH (Fig. 7).

Fig. 7a shows cyclic voltammograms for the modified GCE in absence and increasing the concentration of NADH. The solid line shows the anodic response of two-electron oxidation of the arylhydroxylamine moieties and the corresponding electro-reduction processes (system II). On one side, an enhancement of the anodic current peak at ca. 0.12 V and a decrease in the cathodic wave are clearly observed upon addition of NADH. On the other, it is important to notice that the potential at which this electrocatalytic reaction takes place is shifted 480 mV with respect to the non-catalyzed reaction, which typically takes place at about 0.60 V. For comparison purposes, cyclic voltammograms obtained with an unmodified electrode in the absence and presence of NADH are also shown (Fig. 7b). There is no evidence of anodic peaks, which indicates that the direct oxidation of NADH is out of these limits. Furthermore, the generation-on-demand of surface-immobilized hydroxylamine product by electrochemically triggered reaction is the responsible of the electrocatalytic effect. The electrocatalytic effect only shows up after the electrochemical reduction of D-NO_2/GCE is reached to form the hydroxylamine compound.

4. Conclusions

In this work, the synthesis of a dendritic molecule (D-NO_2) and its immobilization onto GCE and HOPG was achieved. The functionalization of carbon surfaces with D-NO_2 provides controllable properties for the electrode surface due to multifunctional groups of the molecule. D-NO_2 adsorbs onto carbon surfaces spontaneously by dipping the metal surface in dendron solutions. The cooperative effect of phenyl rings and the multifunctionality of D-NO_2 (containing carboxyl and nitro groups) allow a direct and rapid adsorption of the dendrons onto carbon surfaces. The reduction of the dendron layer generates the hydroxylamine product. The resulting redox-active layer exhibits a well-behaved redox response for the adsorbed nitroso/hydroxylamine couple.

The molecules attached onto the carbon surface form a layer covering the whole surface, but do not block the electron transfer reaction of redox probes like $Ru(NH_3)_6^{3+/2+}$ or $Fe(CN)_6^{3-/4-}$. In addition, the generation-on-demand of surface-immobilized hydroxylamine product by the electroreduction of D-NO_2/GCE has an important electrocatalytic effect in NADH oxidation. This effect, together with the remarkable simplicity of obtaining these films, makes these carbon electrodes a potential important tool as electrocatalysis and biosensing platforms.

Acknowledgments

The authors gratefully acknowledge financial support from CONICET, ANPCyT, and SECYT of Universidad Nacional de Córdoba. J.I.P. thanks CONICET for the fellowship.

Appendix A. Supplementary data

Supplementary data associated with this article can be found, in the online version, at doi:10.1016/j.electacta.2009.02.064.

References

[1] A.W. Bosman, H.M. Janssen, E.W. Meijer, Chem. Rev. 99 (1999) 1665.
[2] B.A. Hermann, L.J. Scherer, C.E. Housecroft, E.C. Constable, Adv. Funct. Mater. 16 (2006) 221.
[3] J.M. Frechet, D.A. Tomalia, Dendrimers and Other Dendritic Polymers, Wiley, West Sussex, 2001.
[4] M. Ballauff, C.N. Likos, Angew. Chem., Int. Ed. 43 (2004) 2998.
[5] D.A. Tomalia, Mater. Today 6 (2003) 72.
[6] V.V. Tsukruk, Adv. Mater. 10 (1999) 253.
[7] G.H. Degenhart, B. Dordi, H. Schonherr, G.J. Vancso, Langmuir 2 (2004) 6216.
[8] G. Cooke, J. Couet, J.F. Garety, C.Q. Ma, S. Mabruk, G. Rabani, V.M. Rotello V.M., V. Sindelar, P. Woisel, Tetrahedron Lett. 47 (2006) 3763.
[9] B. Huang, D.A. Tomalia, J. Luminisc. 111 (2005) 215.
[10] M. Mackay, C.R. Chimie. 6 (2003) 747.
[11] Z. Bo, L. Zhang, Z. Wang, X. Zhang, J. Shen, Mater. Sci. Eng. C 10 (1999) 165.
[12] F. Zeng, S. Zimmerman, S. Kolatuchin, D. Reichert, Tetrahedron 58 (2002) 825.
[13] D. Smith, A. Hist, C. Love, J. Hardy, S. Brignell, B. Huang, Prog. Polym. Sci. 30 (2005) 220.
[14] L. Zhu, G. Zhu, M. Li, E. Wang, R. Zhu, X. Qi, Eur. Polym. J. 38 (2002) 2503.
[15] A. Ras, J. Zhen, W. Liu, J. Barnard, A. Bennet, S. Street, Appl. Surf. Sci. 176 (2001) 134.
[16] D. Tzalis, Y. Tor, Tetrahedron Lett. 37 (1996) 8293.
[17] Z. Liu, X. Wang, H. Wu, C. Li, J. Colloid Interface Sci. 287 (2005) 604.
[18] M. Martinelli, M. Calderón, M.C. Strumia, Reactive Funct. Polym. 67 (2007) 1018.
[19] Z.M. Liu, Y. Yang, H. Wang, Y. Liu, G. Shen, R. Yu, Sens. Actuators B 106 (2005) 394.
[20] A. Li, F. Yang, Y. Ma, X. Yang, Biosens. Bioelectron. 22 (2007) 1716.
[21] Y. Zeng, Y. Huang, J. Jiang, X. Zhang, C. Tang, G. Shen, R. Yu, Electrochem. Commun. 9 (2007) 185.
[22] C.M. Yam, M. Deluge, D. Tang, A. Kumar, C. Cai, J. Coll. Interface Sci. 296 (2006) 118.
[23] M. Yang, E.M.W. Tsang, Y.A. Wang, X. Peng, H. Yu, Langmuir 21 (2005) 1858.
[24] L. Zhang, F. Huo, Z. Wang, L. Wu, X. Zhang, S. Hoppener, L. Chi, H. Fuchs, J. Zhao, L. Niu, S. Dong, Langmuir 16 (2000) 3813.
[25] Y. Jiang, Z. Wang, X. Yu, F. Shi, H. Xu, X. Zhang, M. Smet, W. Dehaen, Langmuir 21 (2005) 1986.
[26] A. Rochefort, J.D. Wuest, Langmuir 25 (2009) 210.
[27] J.I. Paez, P. Froimowicz, M.C. Strumia, A.M. Baruzzi, V. Brunetti, Electrochem. Commun. 10 (2008) 541.
[28] J. Wang, Analytical Electrochemistry, VCH Publishers, Inc., USA, 1994.
[29] P. Froimowicz, Ph. D. Diss., Universidad Nacional de Córdoba, Argentina, 2005.
[30] P. Froimowicz, J.I. Paez, A. Gandini, N. Belgacem, M.C. Strumia, Macromol. Symp. 245 (2007) 51.
[31] Y. Ishida, M. Jikei, M. Kakimoto, Macromolecules 33 (2000) 3202.
[32] L. Horcas, R. Fernandez, J.M. Gomez-Rodriguez, J. Colchero, J. Gomez-Herrero, A.M. Baro, Rev. Sci. Instrum. 78 (2007) 013705.
[33] E. Casero, M. Darder, K. Takada, H.D. Abruña, F. Pariente, E. Lorenzo, Langmuir 15 (1999) 127.
[34] X.Y. Xiao, S.G. Sun, Electrochimica Acta 45 (2000) 2897.
[35] A.T. Masheter, L. Xiao, G.G. Wildgoose, A. Crossley, J.H. Jones, R.G. Compton, J. Mater. Chem. 17 (2007) 3515.
[36] G.G. Wildgoose, S.J. Wilkins, G.R. Williams, R.R. France, D.L. Carnahan, L. Jiang, T.G.J. Jones, R.G. Compton, Chem. Phys. Chem. 6 (2005) 352.
[37] B. Ortiz, C. Saby, G.Y. Champagne, D.J. Beïlanger, Electroanal. Chem. 455 (1998) 75.
[38] N. Mano, A.J. Kuhn, Electroanal. Chem. 477 (1999) 79.
[39] Th. Doneux, M. Steichen, T. Bouchta, Cl.J. Buess-Herman, J. Electroanal. Chem. 599 (2007) 241.
[40] H.-Z. Yu, C.-Y. Luo, C.G. Sankar, D. Sen, Anal. Chem. 75 (2003) 3902.
[41] A.O. Solak, L.R. Eichorst, W.J. Clark, R.L. McCreery, Anal. Chem. 75 (2003) 296.
[42] H.M. Nassef, A.E. Radi, C.K. O'Sullivan, Electrochem. Commun. 8 (2006) 1719.
[43] H.M. Nassef, A.E. Radi, C.K. O'Sullivan, J. Electroanal. Chem. 592 (2006) 139.
[44] P. Abiman, G.G. Wildgoose, R.G. Compton, Electroanalysis 19 (2007) 437.
[45] P.R. Lima, W.J.R. Santos, R.C.S. Luz, F.S. Damos, A.B. Oliveira, M.O.F. Goulart, L.T.J. Kubota, Electroanal. Chem. 612 (2008) 87.